第51卷第7期 中国科学技术大学学报 Vol. 51, No. 7
2021年7月 JOURNAL OF UNIVERSITY OF SCIENCE AND TECHNOLOGY OF CHINA Jul. 2021
Received: 2021-01-28; Revised: 2021-04-05 doi:10.52396/JUST-2021-0065

# A novel hybrid solar preheating intercooled gas turbine based on linear Fresnel reflector

Yousef N. DABWAN[1,2], PEI Gang[1*], Trevor Hocksun KWAN[1], ZHAO Bing[1]
1. Department of Thermal Science and Energy Engineering, University of Science and Technology of China, Hefei 230027, China;
2. Department of Mechanical Engineering, Sana'a University, Sana'a, Yemen.
* Corresponding author. E-mail: peigang@ustc.edu.cn

**Abstract**: In this study, a new hybrid Solar Preheating Intercooled Gas Turbine (SPIcGT) is originally introduced, in which a linear Fresnel solar field used for preheating the compressed air before entering the combustor. The solar Preheating Gas Turbine (SPGT) has been used as a reference gas turbine cycle. Eight performance indicators have been used in the analysis under Guangzhou (China) weather data. The study reveals that the SPIcGT is superior to the SPGT system as it is capable of boosting the fuel-based efficiency by 19.5% versus 0.26% for the SPGT system. The SPIcGT has lower specific fuel consumption (about 7017 kJ/kWh) compared with the 10358 kJ/kWh for SPGT. Meanwhile, the solar integration of the linear Fresnel solar field into an intercooled gas turbine cycle is more economical than the solar integration with the conventional gas turbine cycle. The levelized electricity cost of 4.34US$/kWh was achieved for SPIcGT which is lower than 5.15% for SPGT. Moreover, the fuel consumption and $CO_2$ emissions can be reduced greatly (about 19.3%) by integrating the linear Fresnel solar field with the intercooled gas turbine.

**Keywords**: gas turbine; hybrid solar gas turbine; intercooled gas turbine; linear fresnel reflector; solar energy
**CLC number**: TU459 **Document code**: A

## 1 Parameters explaination

Nomenclature

| | |
|---|---|
| $F_{ann}$ | Annual cost of the fuel consumption (US $) |
| $f_{cr}$ | Annuity factor (-) |
| $h$ | specific enthalpy (kJ/kg) |
| $I_{tot}$ | Total investment cost (US $) |
| $K_{insurance}$ | Annual insurance rate (%) |
| $K_d$ | Interest rate (%) |
| LHV | lower heating value (kJ/kg) |
| $\dot{m}$ | mass flow rate (kg/s) |
| $n$ | Depreciation period (Year) |
| $\dot{Q}$ | heat rate (kW) |
| $\dot{w}$ | power (kW) |

Greek letters

| | |
|---|---|
| $\eta$ | efficiency (%) |

Subscripts

| | |
|---|---|
| ann | annual |
| aux | auxiliary |
| c | compressor |
| cc | combustion chamber |
| ch | chemical |
| $e$ | exit |
| en | energy |
| $i$ | inlet |
| net | net |
| $o$ | outlet |
| tot | total |
| ref | reference |

Abbreviation

| | |
|---|---|
| GE | General electric company |
| GT | gas turbine |
| HPC | high pressure compressor |
| HPT | high pressure turbine |
| IcGT | Intercooled gas turbine |
| LEC | Levelized electricity Cost |
| LPC | low pressure compressor |
| LPT | low pressure turbine |
| OM | operation and maintenance costs |
| LFR | linear Fresnel reflector |

**Citation**: DABWAN Y N, PEI Gang, KWAN T H, et al. A novel hybrid solar preheating intercooled gas turbine based on linear Fresnel reflector. J. Univ. Sci. Tech. China, 2021, 51(7): 505-520.

| | |
|---|---|
| SLEC | polar levelized electricity cost |
| SS | annual solar share |
| SP | solar preheating |
| SPGT | solar preheating gas turbine |
| SPIcGT | solar preheating intercooled gas turbine |
| Ref | reference plant |
| US $ | US Dollar |
| US¢ | US cents; ¢ = $ 0.01 |

## 2 Introduction and background

Solar energy resource becomes an attractive option to integrate with a conventional power plant. A hybrid solar power plant is a promising technology that can realize hybrid operations and dispatchability. Medium temperature solar collector systems, such as Linear Fresnel Reflector (LFR), can be used to integrate solar thermal power into a gas turbines[1]. The LFR is simpler and cheaper than the solar tower system and/or parabolic trough collectors[2]. It might provide the method to raise the competitiveness of solar electrical power without the need for high concentration and high temperature in the solar field[3].

Solar energy can be integrated into gas turbine power plants in four main integration concepts as presented in Fig. 1. The first concept (Scheme 1) is to use solar energy to produce steam injected into the combustor. The steam injection increases the power output and efficiency of a gas turbine by increasing the mass flow through the turbine. The solar integration of concentrated solar thermal technology in scheme 1 has been well studied by many researchers. For example, Kribus et al[4-8], performed several studies on hybrid solar steam-injected gas turbine systems. In their proposed systems, steams generated by using the solar energy are injected into the combustion chamber to improve the power output and efficiency. The authors have conducted the thermo-economic analysis for a wide range of operating parameters under different weather conditions. The addition of 4 hours' solar energy storage to the hybrid solar steam-injected gas turbine system[8] increases the capacity factor to more than 50% while adding stability to power output. Ni, et al[9] performed thermodynamic analysis on a solarized gas turbine system with two-stage fuel reforming. Their results showed that the solarized gas turbine system has good thermodynamic performance with high exergy efficiency, He, et al[10] proposed a hybrid solar steam-injected gas turbine cycle with novel water and heat recovery. Their results showed that the system efficiency was increased by 17%. Bianchini, et al[11] combined a solar methane steam reforming technology with a gas turbine system to produce syngas. The mixture of solar syngas and natural gas (generally composed of water steam and hydrogen) from steam reforming reaction is used to feed the gas turbine. The cost and fuel savings reached about 2.7% and 20%, respectively, compared to conventional gas turbine power cycles with direct fossil fuel combustion[11,12].

The solar integration with exhaust gasses (or with bottoming cycle) of the gas turbine (scheme 4) has also been studied well. For example, Dabwan and Mokheimer[1,3,13-15] completed a comprehensive investigation of the technical, economic, and environmental feasibility of integrating a solar energy with gas turbine combined cycles. Their simulation results proved that the integration of solar energy with conventional gas turbine combined cycles is a promising technology of techno-economic feasibility. Li and Yang[16] conducted a study onthe thermo-economic performance of a hybrid solar combined cycle power plant with two pressure levels of solar field. Zhu et al[17] developed a model of solar gas turbine combined cycle with of three pressure levels of solar integration. Adibhatla and Kaushik[18] performed thermo-economic analysis on an integrated solar combined cycle plant. Wang and Yang[19] presented a hybrid solar strategy of a solar trigeneration power plant. Bellos, et al[20] presented energy, exergy and economic evaluation of a solar driven trigeneration power plant.

Concerning scheme 3, the solar energy integration at the inlet of the gas turbine. In this regard, solar energy is utilized to drive the inlet air cooling systems to cool down the inlet air of a gas turbine. Popov[21] used Thermoflow software for comparing two solar integration concepts of a hybrid solar combined cycle plant. Matjanov[22] presented the impact of intake air cooling of a gas turbine combined cycle on the plant performance. The absorption chiller, which proposed to cool the inlet air, is investigated to use three types of heat sources including the solar energy.

In Scheme 2, the solar integration of the solar tower system and/or parabolic trough system between the compressor and the combustion chamber has also been studied well in previous studies. For example, Behar[23] used parabolic trough solar field to preheat the pressurized air of the solar hybrid gas turbine. His results revealed that a solar-to-electric efficiency of 17% is achievable and the compressor ratio has a highly effect on the cycle performance. Wang et al[24] complete the rmo-economic analysis of a solarized gas turbine combined cycle. The parabolic trough system is used to preheat compressed air before its introduction into the combustion chamber. The authors reported that the plant energy efficiency was 24.9% in the cooling mode and 25.7% in the heating mode. However, the solar integration of LFR in Scheme 2, between the compressor outlet and the combustion chamber inlet,

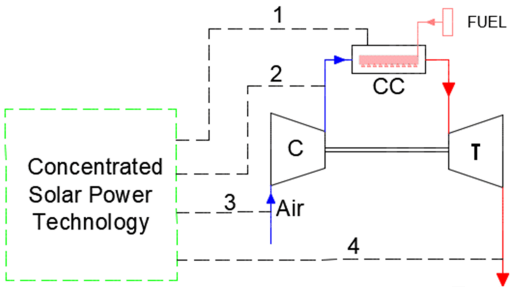


**Figure 1.** Schemes of integrating solar thermal technologies with a gas turbine.

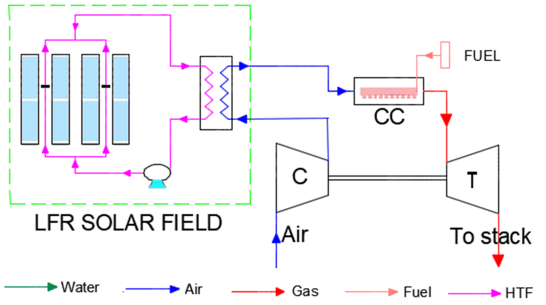


**Figure 2.** Schematic diagram of the solar preheating gas turbine.

has never been reported in the literature.

Based on the literature cited above and to the best of the authors' knowledge, none of the previous studies has considered the integration of linear Fresnel solar field with the intercooled gas turbine cycle. In addition, the vast majority of studies have considered only thermodynamic aspects of using solar technologies in gas turbines without economic features, making the obtained results difficult to generalize. The current study considers both stated gaps and provides a novel contribution to the field of the solar hybrid gas turbine power system. Therefore, in this article, a novel solar hybrid intercooled gas turbine cycle is presented and compared from the thermodynamic and economic points of view. The solar energy collected by the linear Fresnel solar field working with molten salt is used to preheat the compressed air before entering the combustor. The performance of the proposed configuration was annually investigated under the climatic conditions of Guangzhou, China. The proposed novel cycle was compared with the conventional solar preheating gas turbine cycle.

## 3 Configurations

### 3.1 Reference gas turbine cycle

Figure 2 shows a schematic diagram of reference solar preheating gas turbine (SPGT) cycle. In the SPGT configuration, the compressed air is preheated by the linear Fresnel solar field before entering the combustion chamber, where the fossil fuel is completely burned in this compressed air to reach a fixed turbine inlet temperature (1327℃). The flue gases with high energy content are then expanded through gas turbines. General Electric GE6111FA[25,26] has been selected as a conventional gas turbine. The main design parameters of the conventional gas turbine (GE 6111FA) and the solar preheating gas turbine cycle (SPGT) are specified in Table 1.

As known in thermodynamics, the compressor's outlet temperature is strongly affected by the compression ratio. Figure 3 illustrates the compressor outlet temperature versus the compressor pressure ratio for a simple gas

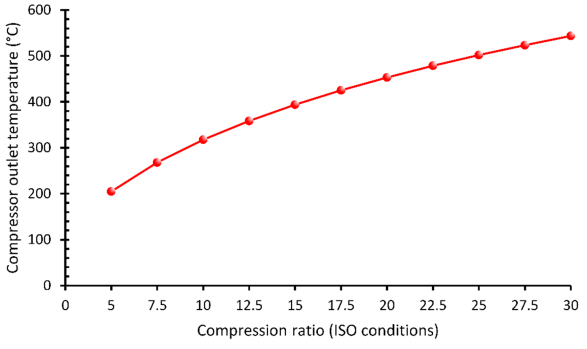


**Figure 3.** The relationship between compressor outlet temperature and compression ratio in a simple gas turbine cycle.

turbine cycle. As shown in the Figure 3, the higher the compression ratio the higher the temperature of the air at the combustion chamber outlet. For example, the compressor outlet temperature is about 453℃ for the cycle with the compression ratio of 20 %. Therefore, the solar integration of the linear Fresnel solar field into a simple gas turbine cycle for preheating the compressed air before combustor seems to be infeasible, especially compressors with high compression ratios. This is because the air temperature at the outlet of the compressor exceeds the maximum operating temperature of the heat transfer fluid in the linear Fresnel solar field. This issue has been solved in this study by integrating the linear Fresnel into the intercooled gas turbine cycle.

### 3.2 Solar preheating intercooled gas turbine cycle

The schematic diagrams of solar preheating intercooled gas turbine cycles (SPIcGT) are presented in Figure 4. The gas turbine unit has a high pressure ratio (1∶37) and intermediate air cooling during compression (Figure 4). In the SPIcGT cycle, the air leaving the low pressure compressor (LPC) is cooled to about 37° C in a primary intercooling system before entering the high pressure compressor (HPC-A). The heat extracted from the compressed air is transferred to the water, which in turn transfers it to the atmosphere through the cooling towers. Cooled air entering the HPC-A is then compressed up to the 13.42 bar. This pressurized air is

**Table 1.** Design parameters of four gas turbine cycles.

| Parameter | GE6111FA (GT) | SPGT | LMS100 (IcGT) | SPIcGT | Comment |
|---|---|---|---|---|---|
| Inlet air mass flow rate (kg/s) | 210 | 210 | 225 | 225 | assumed |
| Inlet pressure loss (bar) | 1% | 1% | 1% | 1% | Evaluated from public data[27] |
| Exist pressure loss (bar) | 1% | 1% | 1% | 1% | Evaluated from public data[27] |
| C/LPC pressure ratio | 15.5∶1 | 15.5∶1 | 3.6∶1 | 3.6∶1 | Evaluated from public data[28-30] |
| C/LPC polytrophic efficiency | 90% | 90% | 90% | 90% | assumed |
| C/LPC, HPC-A, HPC-B mech. Efficiency | 99.2 % | 99.2% | 99.2% | 99.2% | assumed |
| Intercooler pressure loss | – | – | 6% | 6% | Evaluated from public data[27,30] |
| Effectiveness (design) | – | – | 90% | 90% | References[26,29] |
| HPC-A pressure ratio | – | – | 3.9∶1 | 3.9∶1 | Evaluated from public data[28-30] |
| HPC-A and HPC-B polytrophic eff. | – | – | 92% | 92% | assumed |
| HPC-B pressure ratio | – | – | 2.762∶1 | 2.874∶1 | Evaluated from public data[28-30] |
| Mech. eff. of HPC-A and HPC-B compressor | – | – | 99.2% | 99.2% | assumed |
| Combustion chamber pressure loss | 4% | 4% | 4% | 4% | Evaluated from public data[30-32] |
| Combustion chamber heat loss dQ/Q | 0.4% | 0.4% | 0.4% | 0.4% | Evaluated from public data[30,31] |
| Combustion chamber eff. (%) | 99.2% | 99.2% | 99% | 99% | Evaluated from public data[32,33] |
| Combustor outlet temperature ℃ | 1327 | 1327 | 1399 | 1399 | Evaluated from public data[34] |
| Uncooled isentropic eff. of HPT-A, HPT-B, LPT-A, LPT-B. | – | – | 93% | 93% | Evaluated from public data[28,32] |
| Mech. eff. of HPT-A, HPT-B, LPT-A, LPT-A | – | – | 99.2% | 99.2% | Assumed |
| Power turbine polytrophic eff. | 90% | 90% | 93.5% | 93.5% | Assumed |
| Power turbine Mech. eff. | 99.2 % | 99.2% | 99.2% | 99.2% | Assumed |
| Generator eff. | 98.5% | 98.5% | 98.5% | 98.5% | Assumed |

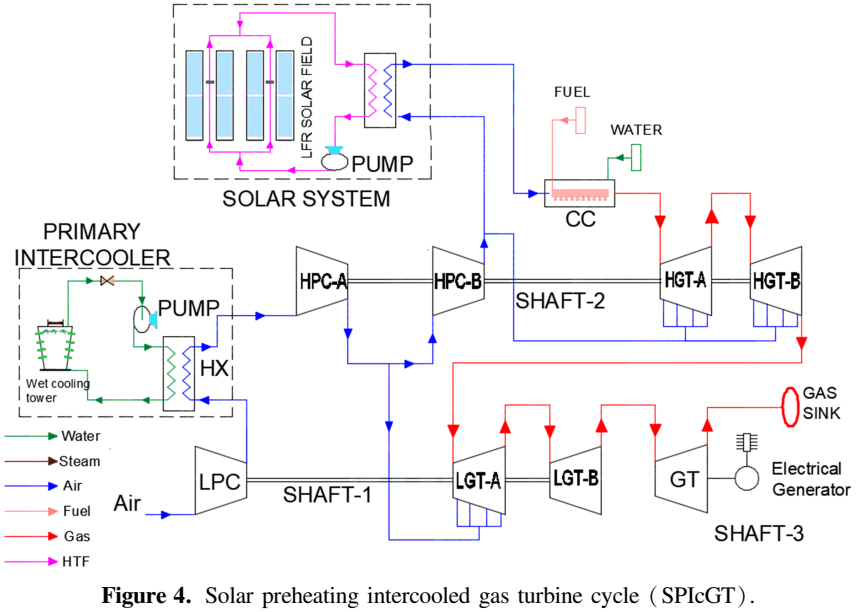


**Figure 4.** Solar preheating intercooled gas turbine cycle (SPIcGT).

then compressed up by HPC-B to the required compressor outlet pressure (37.07 bar). The compressed air from HPC-B is then heated up by the thermal heat obtained by a linear Fresnel solar field before entering the combustion chamber, where the fossil fuel is completely burned in this compressed air to reach a fixed turbine inlet temperature (1399℃). The flue gases with high energy content are then expanded though air cooled gas turbines. The flow flue gases with high-temperature on the turbine blades can cause damages and sometimes creep failure. Therefore, in this study, the stator and rotor of the turbines are cooled by compressed air in order to avoid severe damages. The operation of the intercooled gas turbine cycle differs from the simple gas turbine cycle. In an intercooled gas turbine cycle, an intercooling system is used between two compressors. This intercooler leads to increase the net power output by saving the corresponding amount of compression work. Therefore, General Electric LMS100 has been selected as a reference cycle[28,29,34,35]. The LMS100 is selected because of its added design (intercooling) and size. The SPIcGT cycle is similar to the General electric intercooled gas turbine GE's LMS100, except that there is a solar field in the SPIcGT. In the LMS100 gas turbine, water added to the combustion chamber to increase the power output and efficiency of the gas turbine by increasing the mass flow through the turbine. The main design parameters of the gas turbine cycles (SPGT, LMS100, and SPIcGT) are specified in Table 1. These performance parameters are assumed based on typical standards and best practice from literature.

The module of the Novatec Solar's linear Fresnel reflector design (superheating section)[1] is used in the present study. Table 2 presents the geometrical parameters of the linear Fresnel reflector. The collectors are placed to rotate around a horizontal North-South axis and tracking the sun from East to West.

**Table 2.** Specifications of the linear Fresnel collector[1].

| Parameter | Value |
|---|---|
| Receiver outside diameter(mm) | 70 |
| Receiver wall thickness(mm) | 4.191 |
| Optical efficiency at 0 degrees incidence(%) | 67 |
| Reflector aperture width(m) | 12 |
| Reflector unit width(m) | 16.56 |
| Reflector focal length(m) | 7.4 |
| Aperture with / collector unit width0.7246 | |
| Reflector cleanliness factor | 0.95 |
| Active reflector length as present of total length(%) | 95 |

# 4 Operating parameters and performance criteria

The thermodynamic, economic and environmental performance metrics of the proposed configurations are presented briefly hereunder. Eleven performance parameters were selected to evaluate the plants' performance. The definition and significant of these performance criteria are presented and discussed below:

## 4.1 Overall analysis

The principles of mass and energy conservation applied to any steady state operated control volume are presented hereunder[36].

$$\sum \dot{m}_i = \sum \dot{m}_e \tag{1}$$

$$\dot{Q} + \sum \dot{m}_i h_i = \dot{W} + \sum \dot{m}_e h_e \tag{2}$$

## 4.2 Energy efficiency

It is the ratio of the delivered usable energy (electric power) to the overall energy input to the system (fossil fuel + solar energy). It is given mathematically as[23,37-39]

$$\eta_{\text{en,overall}} = \frac{\dot{W}_{\text{net}}}{\dot{Q}_{\text{fuel}} + \dot{Q}_{\text{solar}}} \tag{3}$$

$W_{net}$ is the net electric power generation.

$$\dot{W}_{\text{net}} = \dot{W}_{gt,shaft} - \dot{W}_{c,\text{shaft}} - \dot{W}_{\text{aux,shaft}} \tag{4}$$

$$\dot{Q}_{\text{fuel}} = \dot{m}_{\text{fuel}} \times \text{LHV} \tag{5}$$

$\dot{m}_{fuel}$ and LHV are the fuel mass flow rate and fuel lower heating value.

## 4.3 Fuel-based efficiency

It is defined as the ratio of electrical power generated from the system to the overall energy from the fuel. In this concept, solar thermal energy is considered free. The equation form can be written as[23]

$$\eta_{fuel-based} = \frac{\dot{W}_{\text{net}}}{\dot{Q}_{\text{fuel}}} \tag{6}$$

## 4.4 Solar heat fraction or solar multiple (SM)

It is the percentage of the total thermal energy satisfied by the solar energy input under design conditions[23,15,40-42].

$$\text{SM} = \frac{\dot{Q}_{\text{solar}}}{\dot{Q}_{\text{fuel}} + \dot{Q}_{\text{solar}}} \tag{7}$$

## 4.5 Incremental carbon dioxide avoidance

It defines as the reduction in $CO_2$ emissions due to the solar energy utilization, It is given as[13,15,41,42]

$$\Delta\text{CO}_2(\%) = \frac{\text{CO}_{2\text{ref}} - \text{CO}_{2\text{hybird}}}{\text{CO}_{2\text{ref}}} \times 100 \tag{8}$$

## 4.6 Fuel saving fraction

It is defined as the percentage of fuel reduction due to the solar energy utilization. It is given mathematically as[23]

$$x_{\text{saving}} = \frac{\dot{Q}_{\text{fuel,ref}} - \dot{Q}_{\text{fuel}}}{\dot{Q}_{\text{fuel,ref}}} \tag{9}$$

### 4.7 Specific fuel consumption

It is the amount of fuel consumed by a gas turbine for each unit of the power output. It is given mathematically as[23]

$$sfc = \frac{\dot{Q}_{\text{fuel}}}{\dot{W}_{\text{net}}} \tag{10}$$

### 4.8 Levelized electricity cost

It is the ratio of the total annual cost to the annual electric power produced by the system. It is given mathematically as[41,43-46]

$$\text{LEC} = \frac{I_{\text{tot}} * f_{\text{cr}} + \text{OM}_{\text{ann}} + F_{\text{ann}}}{E_{\text{el,ann}}} \tag{11}$$

$E_{el,\text{ann}}$ is the annual electric power. $I_{\text{tot}}$ is the total investment cost. $\text{OM}_{\text{ann}}$ is the annual operation and maintenance cost. $F_{\text{ann}}$ is the annual fuel cost. $f_{cr}$ is the annuity factor, which can be calculated as

$$f_{\text{cr}} = \frac{K_d * (1 + K_d)^n}{(1 + K_d)^n - 1} + K_{\text{insurance}} \tag{12}$$

$n$ is the depreciation period in years. $K_{\text{insurance}}$ is the annual insurance rate. $K_d$ is the interest rate. Table 3 listing thermo-economic performance parameters from the literature, which are used to evaluate the above-mentioned assessment metrics.

### 4.9 Solar levelized electricity cost

It is the ratio of the solar field cost to the annual electric power produced due to the solar energy input; and it can be given mathematically as[15,42,43,47]

$$\text{SLEC} = \frac{\text{LEC}_{\text{Hybird}} - [(1 - SS) * \text{LEC}_{\text{ref}}]}{} \tag{13}$$

Where SS is the annual solar share, and it is given mathematically as

$$SS = 1 - \frac{(\text{annual fuel consumption/kWh})_{\text{hybird}}}{(\text{annual fuel consumption/kWh})_{\text{ref}}} \tag{14}$$

**Table 3.** Summary of thermo-economic parameters.

| Parameter | Value |
|---|---|
| Depreciation period(Year) | 20 |
| Annuity factor(%) | 0.11955 |
| Cost of fuel(US $/GJ) | 3.75 |
| $K_{\text{insurance}}$(%) | 1% |
| $K_{\text{d}}$(%) | 9 |
| Fixed operation & maintenance cost(US $/$W_{\text{net}}$ in kW/year) | 20 |
| Variable operation & maintenance cost(US $/ kWh) | 0.002 |
| Specific operation & maintenance cost of a solar field)(% from installation cost of solar field in US $) | 1 |

## 5 Validation

The current model of the single intercooled gas turbine cycle was validated with the original equipment manufacturer published data[29,35,48]. This validation was presented in Table 4. Good agreement is observed between the results of the current study and those reported by References [35,48].

In order to check the accuracy of the current model of the conventional gas turbine, we have compared its predictions with the performance of General Electric GE 6111 FA and highlighted in Table5. The design data of this gas turbine (GE 6111 FA, References [25,26]) is presented in Table 1. By inspecting Table 5, one can notice that the current model predicts the performance of the GE 6111 FA gas turbine with higher accuracy.

**Table 4.** Validation results for an intercooled gas turbine.

| Performance Parameters | LMS100[35,48] | Current $\text{IcGT}_{\text{single}}$(LMS100) model | %Error |
|---|---|---|---|
| Ambient temperature(℃) | 15 | 15 | - |
| Relative humidity(%) | 60 | 60 | - |
| Power output(MWe) | 117 | 117.1 | +0.056% |
| Net electric efficiency(%) | 43.5% (at 50Hz)<br>44.3 (at 60Hz) | 43.83 % | 0.76% (at 50Hz)<br>-0.011% (at 60Hz |
| Exhaust gas temperature(℃) | 440 (at 50Hz)<br>432 (at 60Hz) | 429.9 | -2.29 % (at 50Hz)<br>-0.486% (at 60Hz) |
| Exhaust mass flow rate(kg/s) | 234.5 | 234.5 | 0 |

**Table 5.** Validation results for a conventional gas turbine.

| Performance Parameters | GE 6111 FA[25,26] | Current GE 6111 (FA) model | % Error |
|---|---|---|---|
| Ambient temperature℃ | 15 | 15 | – |
| Relative humidity (%) | 60 | 60 | – |
| Power Output(MWe) | 77.600 | 77.478 | −0.157% |
| Net Elec. Efficiency(%) | 35.7 | 35.73 | +0.084% |
| Exhaust gas Temperature(℃) | 594 | 587.2 | −1.18% |
| Air flow rate (kg/s) | 210 | 210 | 0 |
| Gross Heat Rate at Generator Terminals(kJ/kWh) | 10086 | 10076 | −0.099% |

## 6 Weather data

To better understand the proposed cycles, their performance have been examined at weather data in Guangzhou, China. Figure5 illustrates the average hourly weather data in Guangzhou. The temperature is higher than the standard reference temperature (ISO temperature) for all months except sometimes in January, February, and December. The average minimum temperature is 12.7 ℃ in January and the average maximum temperature reaches 31.07 ℃ in July. The relative humidity is also greater than the standard reference humidity (ISO humidity) during a year except sometimes in October, November, and December. Figure 6 presents the solar irradiance in Guangzhou city. The solar time is 11 hours for 7 months in a year (Mar., Apr., May, Jun, Jul, Aug., and Sep.) where it is 7 hours for other five months (Oct., Nov., Dec., Jan., and Feb.).

## 7 Results and discussion

In this section, the results referred to the solar preheating simple gas turbine (SPGT) and solar hybrid preheating intercooled gas turbine (SPIcGT) power plants are reported. At first, the performance of the intercooled gas turbine (IcGT) manufactured by General electric (LMS100, References [29,35,48]) is used as a reference cycle. The conventional gas turbine (GT) manufactured by General electric (GE 6111FA, References [25,26]) is also used as reference of a simple cycle. In this article, a new solar preheating intercooled gas turbine cycle is proposed. The solar energy collected by the linear Fresnel solar field is used to preheat the compressed air before the combustor inlet. The performance of this novel cycle is investigated and compared with reference cycles (General electric LMS100 (IcGT) and, GE 6111 FA (GT)).

The fuel-based and overall efficiencies during the typical days in summer (11 June) and winter (17 January) are illustrated in Figure 7, and Figure 8, respectively. It important to note that the overall efficiency of the solar preheating gas turbine is estimated via applying the first law of thermodynamics; it is the percentage of the net electric power to the overall energy from both the fuel and solar energy. However, the solar thermal energy is considered free in the fuel − based efficiency. Inspecting results in the Figure 7 and Figure 8, one can notice that as the solar radiation intensity is high, the overall energy efficiency of the solar hybrid intercooled gas turbine is low, but in return, the fuel-based efficiency is high. In fact, the fuel saving mode was selected as operating strategy in which the fuel feeding is a function of the total solar energy obtained from the solar system. Compared to the combustion

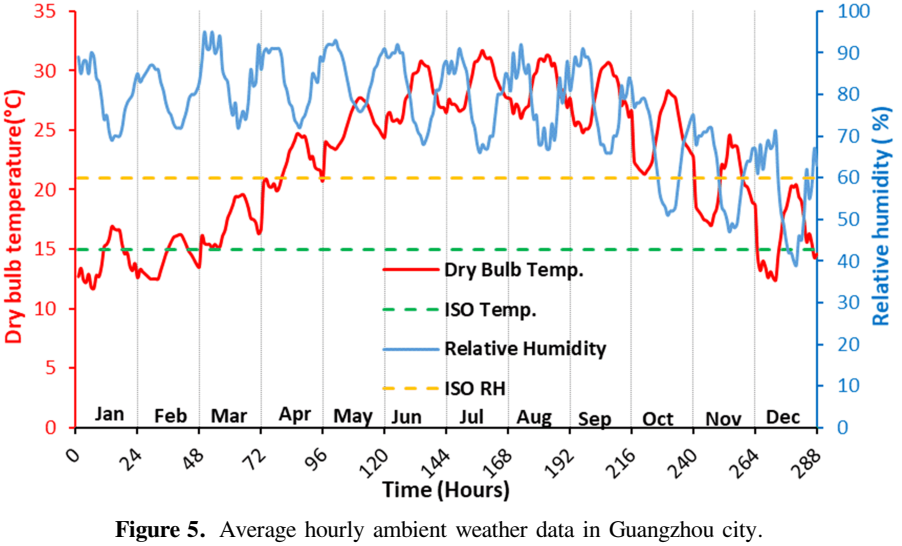


**Figure 5.** Average hourly ambient weather data in Guangzhou city.

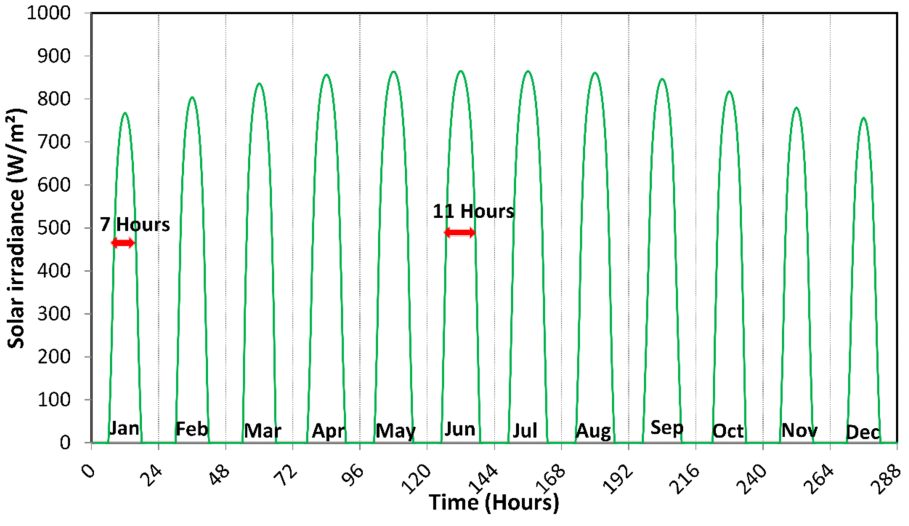


**Figure 6.** Solar irradiance in Guangzhou city, China

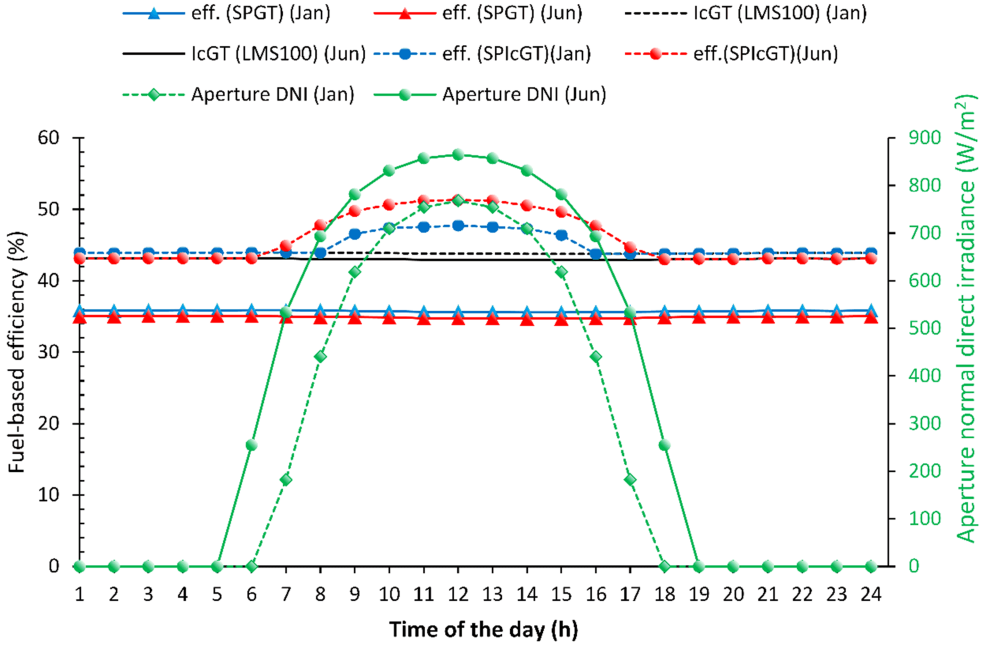


**Figure 7.** Fuel-based efficiency of different conventional and solar hybrid gas turbine plants

process efficiency, solar system has lower thermal efficiency. Therefore, the higher solar energy fraction the lower the overall efficiency. However, the greater the solar energy fraction the lower the consumed fuel, and therefore the higher the fuel-based efficiency becomes. By inspecting Figure 7, one can also notice that the fuel-based efficiency of the SPGT is almost the same as that for GT. This is because the amount of redaction in fuel due to the use of the solar energy is offset by corresponding reduction in net power. Therefore, the change in the value of overall efficiency has remained almost constant.

According to the Figure 8, the net useful solar heat is higher for the case of the solar preheating intercooled gas turbine cycle (SPIcGT) than that of the solar preheating conventional gas turbine cycle (SPGT). This is related to the total solar thermal energy integrated to the cycle which is higher when integrated with SPIcGT due to outlet temperate from the HPC-B. Figure 9 and Figure 10 provide the main solar field performance in both solar hybrid gas turbines at the design hour (midday in June 11). It can be noted that the SPGT does not have an enough opportunity for integrating the solar energy (onl y88. 72 $km^2$ of total aperture area) since the outlet temperature from the compressor is already high (e. g. 431 ℃ in June) and the maximum

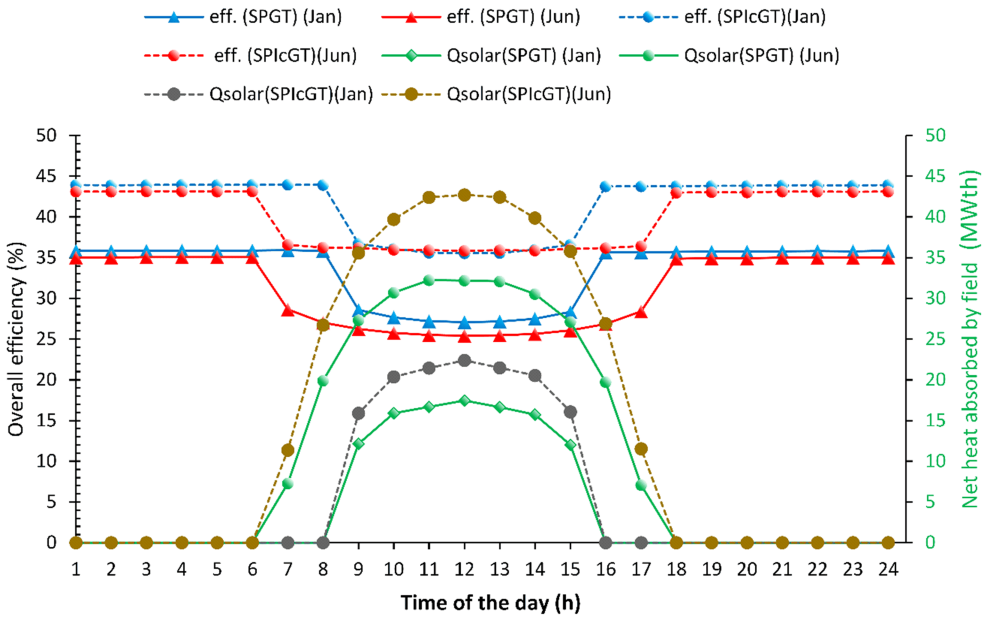


**Figure 8.** Overall efficiency and net solar heat of different conventional and solar hybrid gas turbine plants.

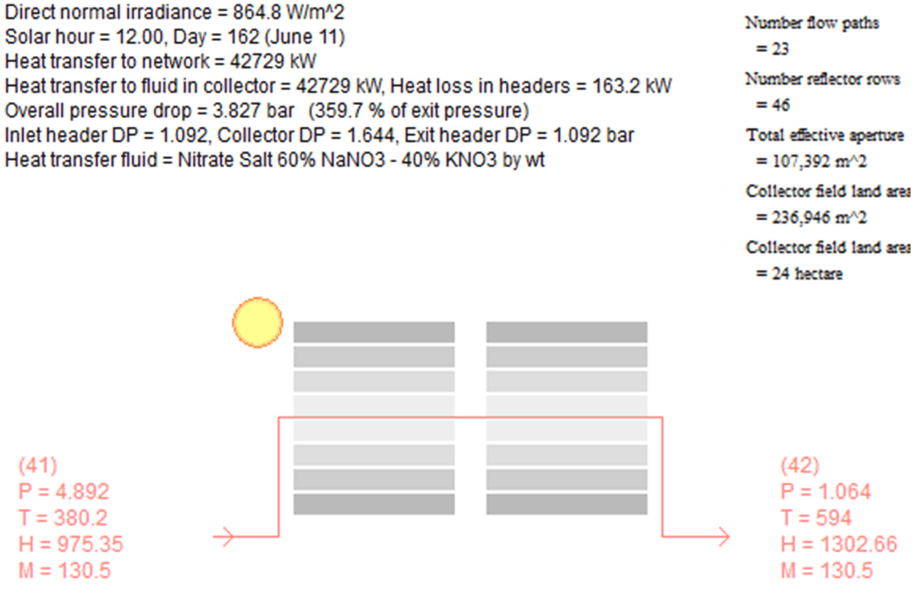


**Figure 9.** Performance of the integrated solar field with intercooled gas turbine at the design hour.

total thermal energy can be integrated with SPGT is low, only about 32 MWth (at midday in summer) of thermal power will be provided by the solar field. However, SPIcGT has an enough room to integrated the solar energy due to the outlet temperature from HPC-B (about 375 ℃). In this regard, the solar integration of the LFR (107.39 km$^2$ of total aperture area) with the SPIcGT produces a thermal power of about 42.72 MWth (15.9% from the total thermal power required from the combustor of 267.96 MWth) at the design hour.

Figure 11, and Figure 12 show the net produced electricity and fuel consumption of the considered gas turbine cycles. It is obvious that the solar integration reduces the produced electricity. This is due to three main reasons: First, the low fuel consumption of the solar hybrid power system leads to the reduction in exhaust gases, thereby reducing the net power of the solar hybrid power system; Second, the pressure losses in the solar heat exchanger require high power consumption; Third, the additional power consumed by the solar pump in the solar hybrid system. Compared to the primary performance of the IcGT cycle (LMS100), the use of LFR with SPIcGT leads to 19.30 % fuel savings with 3.58% reduction in power production.

According to Figure 13, the solar heat and fuel saving rates of the SPIcGT cycle are higher than those

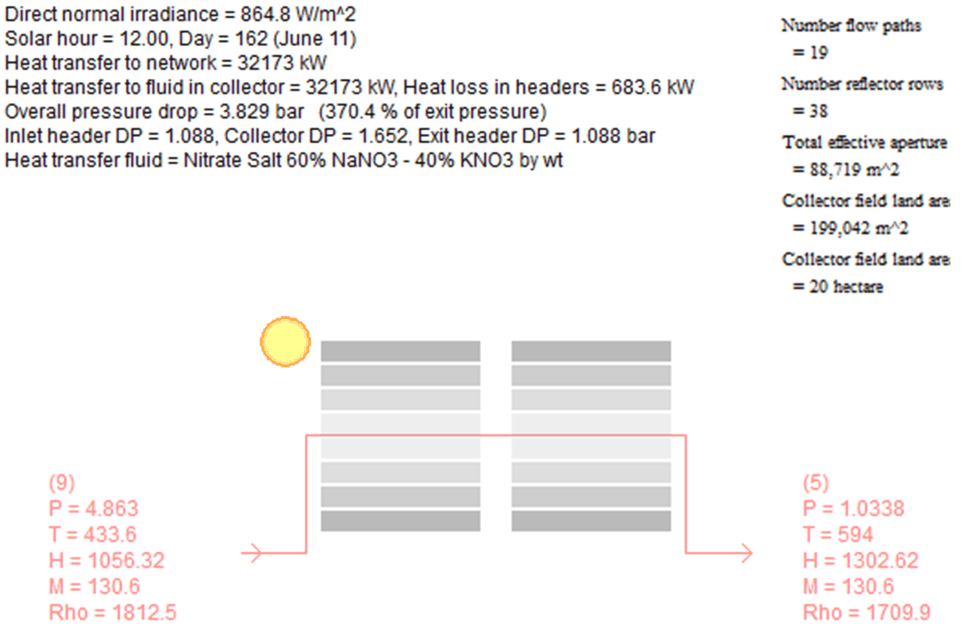


**Figure 10.** Performance of the integrated solar field with conventional gas turbine at the design hour.

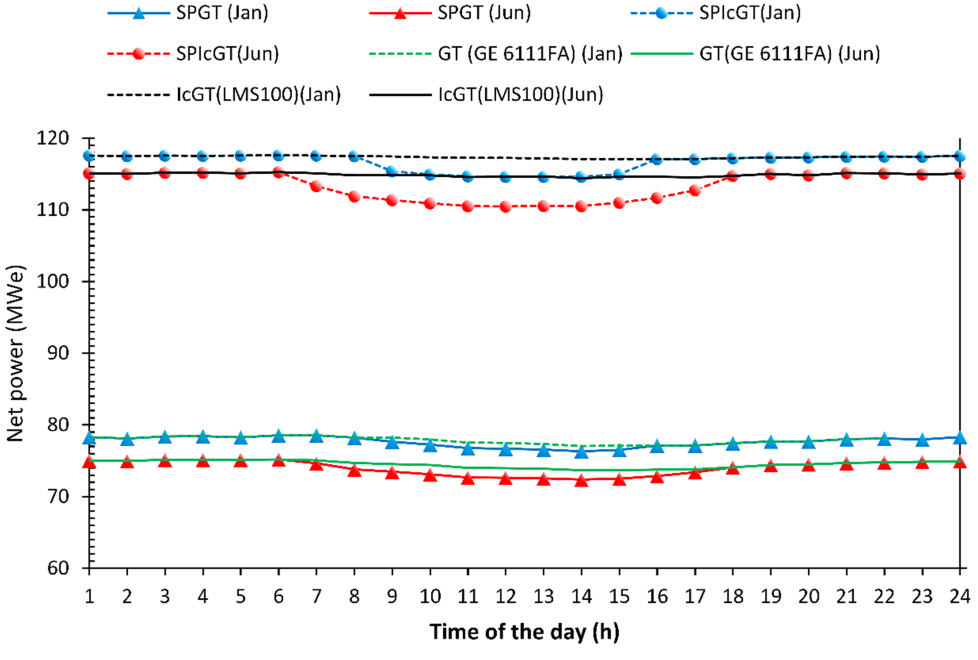


**Figure 11.** Net power of different conventional and solar hybrid gas turbine plants.

of the SPGT. This is due to the higher performance of the LFR integrated with intercooled gas turbine. In the summer, the fuel saving fraction and solar heat ratio are respectively 19. 30% and 16. 43% for the SPIcGT configuration whereas for the SPGT they are in the order of 16. 35% and 13. 06%. Therefore, solar field integration with an intercooled gas turbine results in the comparatively higher values of the $CO_2$ reduction (e. g. 19. 14 % in June) (Figure 14). These results demonstrated that the solar field integration with an intercooled gas turbine might be comparable in cost to the integration of $CO_2$ capturing technology with simple gas turbines.

At an annual operation, the analysis has shown that the summer operation provides better performances than the winter operation for both solar hybrid configurations. The fuel-based and solar heat fractions are both higher in the summer operation than those of the winter operation. This is because the total thermal efficiency of the solar system is higher at the summer

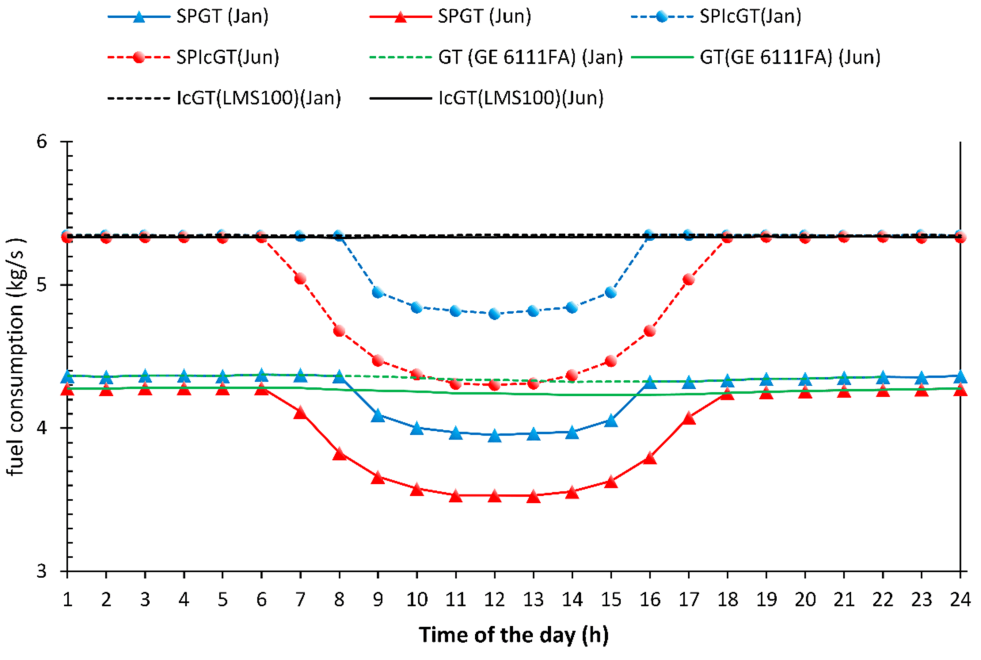


**Figure 12.** Fuel consumption of different conventional and solar hybrid gas turbine plants.

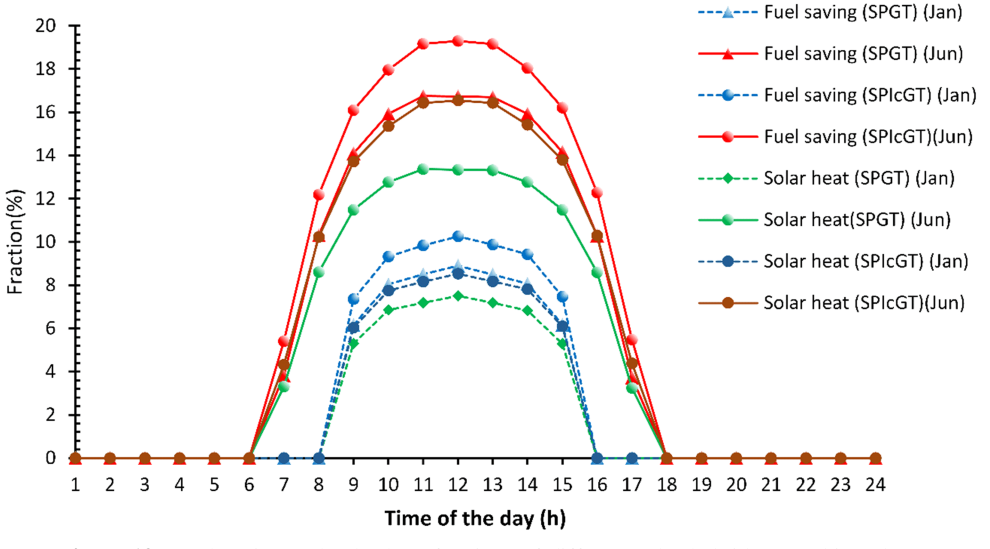


**Figure 13.** Fuel saving and solar heat fractions of different solar hybrid gas turbine plants

operation due to its higher aperture normal direct solar irradiance. As represented in Figure 13, for solar preheating intercooled gas turbine cycle (SPIcGT), fuel saving fraction reaches about 19.3% in the summer session, whereas it is around 9.87% in the winter session.

According to the solar field operating conditions, solar preheating simple gas turbine becomes unfeasible due to the technical limitation linked with the high pressure compressor and solar field working temperatures. However, the intercooling offers a big room for solar integration into modern gas turbine which is featured by the outlet temperature from high pressure compressor. It has been found that the performances of the solar hybrid intercooled gas turbine is better than that of solar hybrid gas turbine. The study revealed that the solar energy integration of LFR with the intercooled gas turbine cycle results in a higher fuel-based efficiency of 51.31% compared to 34.76% for the SPGT. The fuel-based efficiency of the SPIcGT has higher improvement of 47.6% from the SPGT and 19.5% from the LMS100 gas turbine. By looking at Fig. 15, one can notice that the intercooler has a high effect on the specific fuel consumption. In June, the specific fuel consumption is about 7017 kJ/kWh for solar preheating intercooled gas turbine compared with 10358 kJ/kWh for the solar preheating conventional gas turbine. Thus,

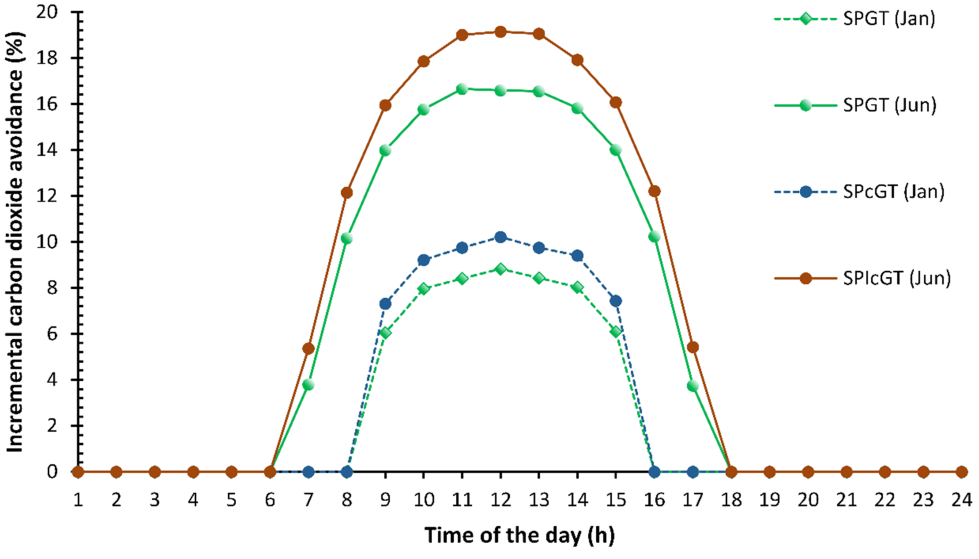


**Figure 14.** Incremental $CO_2$ avoidance of different solar hybrid gas turbine plants.

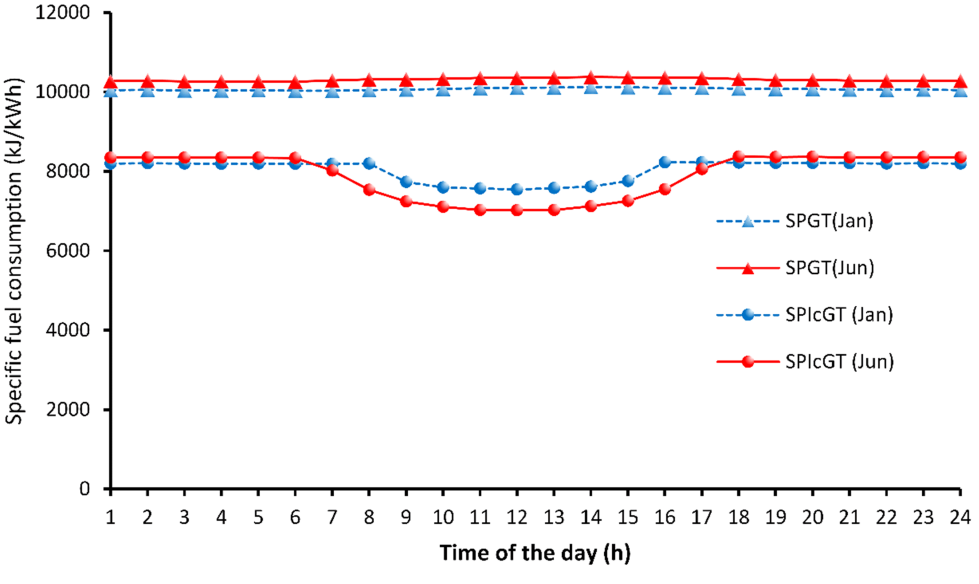


**Figure 15.** Specific fuel consumption of different solar hybrid gas turbine plants.

the solar integration of LFR technology with an intercooled gas turbine is more economic than solar integration with a conventional gas turbine.

The annual reduction of carbon dioxide emissions can be calculated by subtracting the annual $CO_2$ emissions of the solar hybrid gas turbine from the annual $CO_2$ emissions of the conventional gas turbine. By observing Table 6, the solar field integration of LFR with a conventional gas turbine results in a comparatively small value of the annual reduction in $CO_2$ emissions (about 32.5 k-tonne). However, the solar field integration with an intercooled gas turbine results in the relatively high values of the annual avoidance in $CO_2$ emissions (about 45.06 k-tonne). Table 6 also presents the levelized electricity cost (LEC) and solar levelized electricity cost (SLEC) of different solar hybrid preheating gas turbine configurations (SPGT, SPIcGT). By inspecting Table 6, it can be noticed that the solar integration of linear Fresnel solar field with an intercooled gas turbine is more economic than solar integration with a conventional gas turbine.

**Table 6.** Economic and environmental results of the annual operation.

| Configurations | Annual $CO_2$ avoidance (*k*-tonne) | LEC (US¢/kWh) | SLEC (US¢/kWh) |
|---|---|---|---|
| GT (GE 6111FA) | – | 4.66 | – |
| SPGT | 32.50 | 5.15 | 14.7 |
| IcGT (LMS100) | – | 4.01 | – |
| SPIcGT | 45.06 | 4.34 | 10.16 |

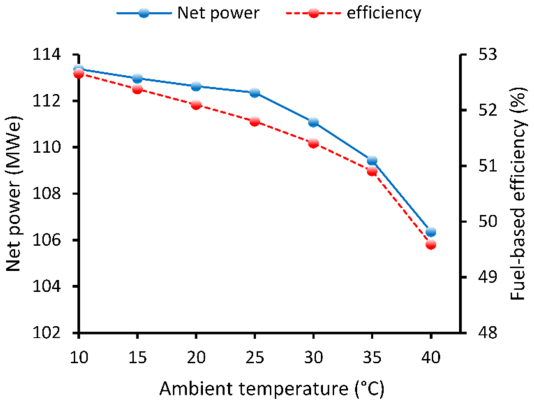


**Figure 16.** Solar preheating intercooled gas turbine performance as a function of ambient temperature (at 864 W/ $m^2$ solar irradiance and at 60 % relative humidity)

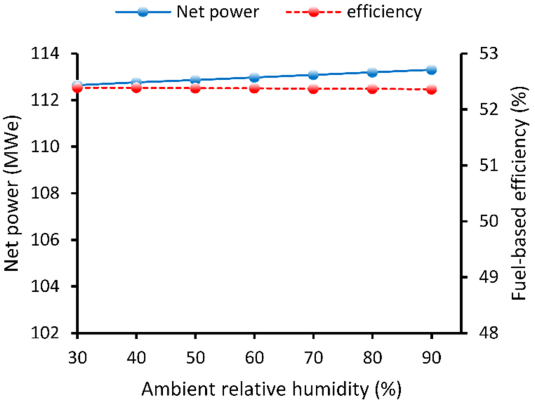


**Figure 17.** Solar preheating intercooled gas turbine performance as a function of relative humidity (at 15 ℃ ambient temperature 15 ℃ and 864 W/ $m^2$ solar irradiance).

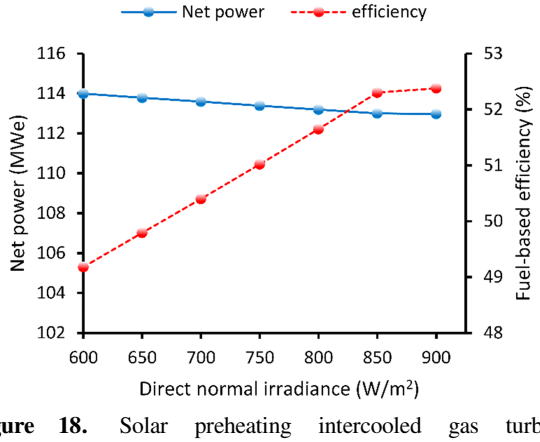


**Figure 18.** Solar preheating intercooled gas turbine performance as a function of solar irradiance (at 15 ℃ ambient temperature and 60% relative humidity).

The performance of solar preheating intercooled gas turbine power plant (SPIcGT) depends on solar irradiance, ambient temperature and relative humidity of the plant. As shown in Figure 16, the net power and fuel-based efficiency are plotted as a functions of ambient temperature at 864 W/ $m^2$ solar irradiance and at 60 % relative humidity. The plant performance indicates a high changes with the variation of ambient temperature. This is because the compressor work is purely a function of air intake temperature, which results in a net reduction in plant net power and plant efficiency. According to the results in Figure 17, the plant performance does not much affected by relative humidity. However, the fuel-based efficiency drops substantially when the solar irradiance decreases more than 800 W/$m^2$ where the net power increases. This behavior occurs as a result of the increase in the fuel consumption resulting from the reduction in solar radiation. In the solar hybrid system, the total required the thermal energy input to be the function of the fuel and solar energy input. Therefore, the lower solar energy input the higher fuel consumption, and thus the lower fuel-based efficiency. For the solar irradiance higher than 800 W/$m^2$, the plant performance indicates a small change with the variation of the solar power input resulting from the varying solar irradiance. This is because the size of the solar field is big and it is not affected by the solar radiation more than 800 W/$m^2$. Moreover, the solar irradiance equal or more than 800 W/$m^2$ is enough for producing the thermal energy required from the solar field where the output temperature from the solar field is about 595 ℃.

## 8 Conclusions

The innovative design of hybrid solar preheating intercooled gas turbine (SPIcGT) is proposed and examined in the current study. In this system, the solar energy is collected by a linear Fresnel solar field is used to preheat the compressed air before entering the combustor. The General electric LMS100 and GE 6111FA have been considered as reference gas turbine cycles. Eight performance parameters have been considered to evaluate the performance of proposed cycles. The following conclusions are obtained:

(Ⅰ) The lower temperature at outlet high pressure compressor offers a big room for the solar integration of the linear Fresnel solar field into the modern gas turbine engine. 19.3% of fuel saving is achieved with annual reduction of 45.06 k-ton in $CO_2$ emissions by integrating linear Fresnel solar field with the intercooled gas turbine system.

(Ⅱ) The solar preheating intercooled gas turbine (SPIcGT) provides a better performance and a lower levelized electricity cost than the solar preheating conventional gas turbine (SPGT). For example, the fuel-based efficiency of about 51.31% can be achieved for SPIcGT with 47.6% improvement from the SPGT and 19.5% from the intercooled gas turbine. The levelized electricity costs of SPIcGT and SPGT are 4.34

US¢/kWh and 5.15 US¢/kWh, respectively.

(Ⅲ) The solar preheating intercooled gas turbine (SPIcGT) has much lower specific fuel consumption (about 7017 kJ/kWh) compared with the 10358 kJ/kWh for the solar preheating conventional gas turbine (SPGT).

(Ⅳ) The solar preheating intercooled gas turbine is a new technology and might be attractive techniques under different climates.

## Acknowledgments

This study was funded by the CAS President's International Fellowship Initiative (2020PE0016) and the National Natural Science Foundation of China (51761145109). This work was also supported by the Fundamental Research Funds for the Central Universities (WK2090000021).

## Conflict of interest

The authors declare no conflict of interest.

## Author information

**PEI Gang** is a Full Professor at University of Science and Technology of China (USTC). He is mainly engaged in research field of comprehensive utilization of solar energy, photoelectricity, and heat. As a visiting scholar, he went to the University of California, Los Angeles, the University of Nottingham, and the City University of Hong Kong for academic visits and exchanges. He has published more than 167 scientific papers with over 3100 total citations (H-index 41). He has 31 authorized invention patents, 2 of which have obtained Geneva International Invention Special Gold Award (the highest award in the exhibition).

**Trevor Hocksun KWAN** is an Australian-born Chinese who was awarded his bachelor (2013/12) and PhD degrees (2017/9) at the University of Sydney. Currently, Dr. Kwan is an associate researcher at the University of Science and Technology of China (USTC). His research interests include thermodynamic analysis, subsystem coupling relationships, and energy management of multi-energy hybrid systems.

**ZHAO Bin** received his PhD degree in University of Science and Technology of China. He is currently a postdoctor in University of Science and Technology of China. His research interests include radiative sky cooling, solar energy harvesting, and spectrally selective coating.

## References

[1] Dabwan Y N, Mokheimer E M. Optimal integration of linear Fresnel reflector with gas turbine cogeneration power plant. Energy Conversion and Management, 2017 148 (Supplement C): 830-843.

[2] Bellos E, Tzivanidis C, Papadopoulos A. Optical and thermal analysis of a linear Fresnel reflector operating with thermal oil, molten salt and liquid sodium. Applied Thermal Engineering, 2018 133: 70-80.

[3] Dabwan Y N, Pei G, Gao G, et al. A novel integrated solar tri-generation system for cooling, freshwater and electricity production purpose: Energy, economic and environmental performance analysis. Solar Energy, 2020, 198: 139-150.

[4] Livshits M, Kribus A. Solar hybrid steam injection gas turbine (STIG) cycle. Solar Energy, 2012, 86(1): 190-199.

[5] Selwynraj A I, Iniyan S, Polonsky G, et al. Exergy analysis and annual exergetic performance evaluation of solar hybrid STIG (steam injected gas turbine) cycle for Indian conditions. Energy, 2015, 80: 414-427.

[6] Selwynraj A I, Iniyan S, Polonsky G, et al. An economic analysis of solar hybrid steam injected gas turbine (STIG) plant for Indian conditions. Applied Thermal Engineering, 2015, 75: 1055-1064.

[7] Selwynraj A I, Iniyan S, Suganthi L, et al. Annual thermodynamic analysis of solar power with steam injection gas turbine (STIG) cycle for indian conditions. Energy Procedia, 2014, 57: 2920-2929.

[8] PolonskyG, Kribus A. Performance of the solar hybrid STIG cycle with latent heat storage. Applied Energy, 2015, 155: 791-803.

[9] Ni M, Yang T, Xiao G, et al. Thermodynamic analysis of a gas turbine cycle combined with fuel reforming for solar thermal power generation. Energy, 2017, 137: 20-30.

[10] He Y, Zheng S, Xiao G. Solar hybrid steam-injected gas turbine system with novel heat and water recovery. Journal of Cleaner Production, 2020, 276: 124268.

[11] Bianchini A, Pellegrini M, Saccani C. Solar steam reforming of natural gas integrated with a gas turbine power plant. Solar Energy, 2013, 96: 46-55.

[12] Bianchini A, Pellegrini M, Saccani C. Solar steam reforming of natural gas integrated with a gas turbine power plant: Economic assessment. Solar Energy, 2015, 122: 1342-1353.

[13] Dabwan Y N, Pei G, Jing L, et al. Development and assessment of integrating parabolic trough collectors with gas turbine trigeneration system for producing electricity, chilled water, and freshwater. Energy, 2018, 162: 364-379.

[14] DabwanY N, Pei G. A novel integrated solar gas turbine trigeneration system for production of power, heat and cooling: Thermodynamic-economic-environmental analysis. Renewable Energy, 2020, 152: 925-941.

[15] Mokheimer E M A, Dabwan Y N, Habib M A, et al. Development and assessment of integrating parabolic trough collectors with steam generation side of gas turbine cogeneration systems in Saudi Arabia. Applied Energy, 2015, 141: 131-142.

[16] Li Y, Yang Y. Impacts of solar multiples on the performance of integrated solar combined cycle systems with two direct steam generation fields. Applied Energy, 2015, 160: 673-680.

[17] Zhu G, Neises T, Turchi C, et al. Thermodynamic evaluation of solar integration into a natural gas combined cycle power plant. Renewable Energy, 2015, 74: 815-824.

[18] Adibhatla S, Kaushik S C. Energy, exergy and economic (3E) analysis of integrated solar direct steam generation combined cycle power plant. Sustainable Energy Technologies and Assessments, 2017, 20: 88-97.

[19] Wang J, Yang Y. A hybrid operating strategy of combined

cooling, heating and power system for multiple demands considering domestic hot water preferentially: A case study. Energy, 2017, 122: 444-457.
[20] Bellos E, Tzivanidis C, Torosian K. Energetic, exergetic and financial evaluation of a solar driven trigeneration system. Thermal Science and Engineering Progress, 2018, 7: 99-106.
[21] Popov D. Innovative solar augmentation of gas turbine combined cycle plants. Applied Thermal Engineering, 2014, 64(1): 40-50.
[22] Matjanov E. Gas turbine efficiency enhancement using absorption chiller: Case study for Tashkent CHP. Energy, 2020, 192: 116625.
[23] Behar O. A novel hybrid solar preheating gas turbine. Energy Conversion and Management, 2018, 158: 120-132.
[24] Wang J, Lu Z, Li M, et al. Energy, exergy, exergoeconomic and environmental (4E) analysis of a distributed generation solar-assisted CCHP (combined cooling, heating and power) gas turbine system. Energy, 2019, 175: 1246-1258.
[25] Power G. Proprietary G E. Fim Proposal. [2021-03-15], http://www.centralesdelacosta.com.ar/ciclo_combinado/PARTE%20II/PARTE%20II%20-%20%20%20ANEXO%20II%20-%20TURBINA%20GE%20FRAME%206FA%20EXISTENTE.pdf, 2012.
[26] Marin G, Osipov B, Mendeleev D. Research on the influence of fuel gas on energy characteristics of a gas turbine. in E3S Web of Conferences. EDP Sciences, 2019, 124: 05063.
[27] Abudu K, Igie U, Roumeliotis I, et al. Aeroderivative gas turbine back-up capability with compressed air injection. Applied Thermal Engineering, 2020, 180: 115844.
[28] Ol'khovskii G G, Radin Y A, Ageev A V, et al. Thermal tests of LMS100 gas-turbine units at the Dzhubga thermal power plant. Power Technology and Engineering, 2016 50(3): 294-302.
[29] Power G. LMS100 * gas turbine (50 Hz). 2015
[30] Walsh P P, Fletcher P. Gas Turbine Performance. John Wiley & Sons, 2004.
[31] Saravanamuttoo H I, Rogers G F C, Cohen H. Gas Turbine Theory. Pearson Education, 2001.
[32] Canière H, Willockx A, Dick E, et al. Raising cycle efficiency by intercooling in air-cooled gas turbines. Applied Thermal Engineering, 2006, 26(16): 1780-1787.
[33] Lefebvre A H, Ballal D R. Gas Turbine Combustion: Alternative Fuels and Emissions. CRC press, 2010.
[34] Reale M J, Prochaska J K. New high efficiency simple cycle gas turbine - GE's LMS100. GER-4222A, GE Energy, 2004.
[35] Power G. LMS100 power plants. General Electric Company, 2019.
[36] Bejan A. Advanced Engineering Thermodynamics. John Wiley & Sons, 2016.
[37] Ellingwood K, Mohammadi K, Powell K. Dynamic optimization and economic evaluation of flexible heat integration in a hybrid concentrated solar power plant. Applied Energy, 2020, 276: 115513.
[38] MishraS, Sanjay Y H. Energy and exergy analysis of air-film cooled gas turbine cycle: Effect of radiative heat transfer on blade coolant requirement. Applied Thermal Engineering, 2018, 129: 1403-1413.
[39] Mishra S, Sharma A, Kumari A, et al. Response surface methodology based optimization of air-film blade cooled gas turbine cycle for thermal performance prediction. Applied Thermal Engineering, 2020, 164: 114425.
[40] Montes M, Abánades A, Martinez-Val J, et al. Solar multiple optimization for a solar-only thermal power plant, using oil as heat transfer fluid in the parabolic trough collectors. Solar Energy, vol. 83, no. 12: 2165-2176, 2009.
[41] Dabwan Y N, G. Pei, G. Gao, J. Li, and J. Feng. Performance analysis of integrated linear fresnel reflector with a conventional cooling, heat, and power tri-generation plant. Renewable Energy, 2019, 138: 639-650.
[42] Mokheimer E M A, Dabwan Y N, Habib M A. Optimal integration of solar energy with fossil fuel gas turbine cogeneration plants using three different CSP technologies in Saudi Arabia. Applied Energy, 2017, 185: 1268-1280.
[43] Dersch J, Geyer M, Herrmann U, et al. Trough integration into power plants: A study on the performance and economy of integrated solar combined cycle systems. Energy, 2004, 29(5): 947-959.
[44] Energy Information Administration. Levelized Cost and Levelized Avoided Cost of New Generation Resources in the Annual Energy Outlook 2018. US, 2018.
[45] Nezammahalleh H, Farhadi F, Tanhaemami M. Conceptual design and techno-economic assessment of integrated solar combined cycle system with DSG technology. Solar Energy, 2010, 84(9): 1696-1705.
[46] Cau G, Cocco D, Tola V. Performance and cost assessment of integrated solar combined cycle systems (ISCCSs) using $CO_2$ as heat transfer fluid. Solar Energy, 2012 86(10): 2975-2985.
[47] Horn M, Führing H, Rheinländer J. Economic analysis of integrated solar combined cycle power plants: A sample case: The economic feasibility of an ISCCS power plant in Egypt. Energy, 2004, 29(5): 935-945.
[48] Power G. Aeroderivative Gas Turbine LMS100. [2021-03-15], https://www.ge.com/gas-power/products/gas-turbines/lms100.

# 一种基于线性菲涅耳反射镜的混合太阳能预热中冷燃气轮机

Yousef N. DABWAN[1,2], 裴 刚[1*], 关学新[1], 赵 斌[1]

1. 中国科学技术大学热能科学与能源工程系,安徽合肥 230027

2 . 也门萨那大学机械工程系,也门萨那

* 通讯作者. E-mail:peigang@ustc.edu.cn

**摘要**: 首次提出了一种新型的混合式太阳能预热中冷燃气轮机(SPIcGT),其利用线性菲涅耳太阳镜场在进入燃烧室前对压缩空气进行预热. 本文以太阳能预热燃气轮机(SPGT)作为参考,采用了八个绩效指标在广州(中国)的天气数据下进行分析. 结果表明,SPIcGT 系统的燃油效率提高了 19.5%,而 SPGT 系统的效率仅提高了 0.26%,因此 SPIcGT 系统优于 SPGT 系统,且与 SPGT 的 10358 kJ/kWh 相比,SPIcGT 有着更低的比油耗(约 7017 kJ/kWh). 同时,线性菲涅耳太阳镜场与中冷燃气轮机循环的太阳能集成比与常规燃气轮机循环的太阳能集成更经济,其电价为 4.34 US$/kWh,比 SPGT 降低了 5.15%. 此外,线性菲 涅耳太阳镜场与中冷燃气轮机的结合可以大大降低燃油消耗和 CO2 排放(约 19.3%).

**关键词**: 燃气轮机;混合太阳能燃气轮机;中间冷却的燃气轮机;线性菲涅耳反射器;太阳能